CO2 column averaged mixing ratio from inversion of ground-based solar spectra

Emanuel Dufour, Francois-Marie Breon, Philippe Peylin

CO_2 column averaged mixing ratio from inversion of ground-based solar spectra

Emmanuel Dufour and François-Marie Bréon
Laboratoire des Sciences du Climat et de l'Environnement, Commissariat à l'Energie Atomique, Gif sur Yvette, France

Philippe Peylin
Laboratoire de Biogéochimie des Milieux Continentaux, INRA Grignon, Thiverval-Grignon, France

Received 18 December 2003; revised 19 February 2004; accepted 25 February 2004; published 12 May 2004.

[1] High resolution sun spectra from the Kitt Peak observatory are used to estimate the column-averaged mixing ratio of carbon dioxide in the atmosphere. Solar absorption lines are apparent on the measured spectra together with the telluric lines. Their discrimination is easy as they are spectrally shifted according to the Earth-Sun relative speed. For the objective of CO_2 mixing ratio estimate, a spectral window of size 15 cm^{-1}, with approximately 10 absorption lines, contains most of the necessary information. The window selection is based on the absence of contamination by other gases and solar absorption lines. Favorable spectral windows are found near 1.6 and 2.0 μm. A radiative transfer model is used to reproduce the data and make the inversion. An excellent fit is obtained. The retrieved CO_2 mixing ratio agrees with the expected values within a few percents and shows the expected growth rate of 1.5 ppm per year. On the other hand, the observed short-term variability of several ppm is much larger than what is expected from simulations by an atmospheric transport model using optimized fluxes. It appears necessary to correct the CO_2 mixing ratio estimates using concomitant measurements of the O_2 mixing ratio, which provides a proxy for the dry air optical path. After the correction, the annual cycle of the CO_2 content above Kitt Peak is apparent on the retrieved values. The comparison of the inverted mixing ratios with the simulation results indicates an error on the order of 1.5 ppm RMS for the 1.6-μm band and 2.5 ppm RMS for the 2.0-μm band. The uncertainty on the effective airmass due to the long acquisition time of the spectra, with varying solar zenith angle, may be responsible for a large fraction of the error. *INDEX TERMS:* 0322 Atmospheric Composition and Structure: Constituent sources and sinks; 0394 Atmospheric Composition and Structure: Instruments and techniques; 1640 Global Change: Remote sensing; 1610 Global Change: Atmosphere; *KEYWORDS:* atmospheric CO_2, spectroscopy, CO_2 absorption

Citation: Dufour, E., F.-M. Bréon, and P. Peylin (2004), CO_2 column averaged mixing ratio from inversion of ground-based solar spectra, *J. Geophys. Res.*, *109*, D09304, doi:10.1029/2003JD004469.

1. Introduction

[2] The prediction of the future rate of increase of atmospheric CO_2 and its impact on global warming is currently hampered by our poor knowledge of the carbon budget. Although net fluxes of CO_2 are relatively well characterized at oceanic basin and continental scale, large uncertainties remain in the regional distribution of the CO_2 sources and sinks around the globe [*Schimel et al.*, 2001]. Indeed, the limited spatial and temporal density of the existing network of CO_2 monitoring stations [*GLOBALVIEW-CO_2*, 2000] makes it difficult to unambiguously relate concentration measurements to surface fluxes below a certain spatial resolution [*Bousquet et al.*, 2000; *Rayner and O'Brien*, 2001].

0148-0227/04/2003JD004469

[3] Global simulations of sources and sinks with inverse transport model [*Rayner and O'Brien*, 2001] have shown that the uncertainty in the CO_2 fluxes determination could be substantially reduced if the current surface network was supplemented by spaceborne measurements of CO_2 column averaged concentrations provided that the latter are individually achieved with a precision of about 1 ppm (0.3%). It is possible to infer CO_2 column densities from space by a spectral, differential absorption analysis of sunlight reflected by the Earth in an absorption band of CO_2. Recently, several theoretical concept studies, based on radiative transfer simulations, have put forward the potential of such a method for meeting the precision requirement imposed by the scientific objectives [*Buchwitz et al.*, 2000; *Dufour and Bréon*, 2003; *Kuang et al.*, 2002; *Tolton and Plouffe*, 2001]. In the near future, dedicated space missions such as the NASA Orbiting Carbon Observatory (OCO) mission should provide mea-

surements of CO_2 column-averaged mixing ratios with sub ppm precisions using the sunlight-based differential absorption technique [*Crisp et al.*, 2002]. Prior to OCO and other similar missions, ground-based column measurements of atmospheric CO_2 concentration are needed to provide a preliminary validation of the spaceborne technique. This paper addresses this objective by investigating the precision that can be reached from ground-based measurements recorded by the McMath-Pierce solar-viewing FTIR spectrometer on Kitt Peak.

[4] In addition, independently of satellite measurements, a column measurement has some advantages to the classical surface continuous or flask sampling. Indeed, in regions of large surface fluxes such as vegetated areas, the CO_2 vertical profile shows a very large vertical gradient that is hardly accounted for in atmospheric transport model, a consequence of difficulties in representing the vertical mixing. The unresolved vertical structure generates some uncertainty when surface measurements are used to infer surface fluxes through atmospheric modeling inversion. A vertical column is much less affected than a surface flask sampling by the uncertainties on the vertical mixing. Therefore column measurements such as proposed in this study may prove attractive to complement the current network of surface measurements.

[5] The retrieval of column-averaged mixing ratio of atmospheric CO_2 from the Kitt Peak observations has been reported twice in the past. In the pioneer study, *Wallace and Livingston* [1990] used the equivalent width technique [*Farmer et al.*, 1980; *Park et al.*, 1980] applied to a selection of isolated CO_2 absorption lines around 1.6 μm together with O_2 absorption lines around 1.27 μm. The O_2 band was used to provide a spectroscopic surrogate for the amount of dry air along the telescope line of sight. More recently, *Yang et al.* [2002] conducted a re-analysis of the Kitt Peak data using a multispecies non-linear least squares fitting method over the entire 1.27-μm and 1.6-μm absorption bands. In their study, *Yang et al.* [2002] managed to recover column-averaged mixing ratios of CO_2 with estimated precisions of better than 0.5% or 1.7 ppm.

[6] Although the present work bears several similarities with the above mentioned papers, it differs by three major aspects: First, an additional spectral interval, lying in the 2.0-μm CO_2 absorption band, is considered in addition to the 1.6-μm CO_2 band and the 1.27-μm O_2 band. Radiative transfer simulations have shown that the 2.0-μm band is necessary on the OCO payload, in addition to the 1.6-μm band, to provide additional constraints on the CO_2 retrievals and on the correction for aerosol scattering effect on the measurements [*Crisp et al.*, 2002; *Kuang et al.*, 2002]. Second, the spectra inversion results are analyzed in comparison to the predictions of an atmospheric transport model, and we discuss the expected differences resulting from short-term variability that may not be fully represented in the model. This permits an objective quantification of the spectra inversion errors. Finally, for a closer simulation of the characteristics of a Fourier Transform spectrometer currently in development at CNES (Centre National des Etudes Spatiales) [*Rosak and Tintó*, 2003], we have intentionally limited the measurements to narrow (15 cm^{-1}) optimized spectral intervals.

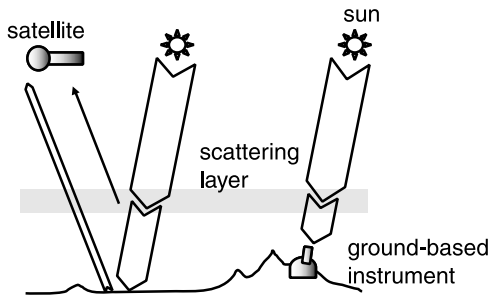

Figure 1. Satellite and ground-based measuring principle. The ground-based measurement, aiming directly at the sun, benefits from a much larger flux in comparison to the spaceborne measurement that uses the reflected sunlight. Scattering material in the atmosphere may attenuate, but does not affect spectrally over a small spectral interval, the direct radiance incoming at the surface. In the satellite case, the presence of a scatterer produces a significant fraction of measured photons that have not traveled through a double atmospheric path. These photons are less absorbed and yield a low bias for the column retrieval.

2. Data and Method

2.1. Basic Measuring Principle

[7] Differential absorption spectroscopy relies on the spectral analysis of the transmission of the solar radiance through the atmosphere. As predicted by Beer-Lambert law, the intensity of the absorption lines of a gas can be directly linked up to its integral amount along the atmospheric path. The latter can be retrieved provided the knowledge of the spectroscopic coefficients of interest together with the thermo dynamical state of the atmosphere (vertical profiles of pressure and temperature). Furthermore, if the total mass of dry air optically traversed is established, one may recover column-averaged concentrations.

[8] The principle of differential absorption can be applied to atmospheric spectra measured by a satellite or from the ground aiming at the sun. In the latter case, the measured sunlight arrives directly to the instrument after a single atmospheric travel whereas in the spaceborne concept, the sun radiance goes through a double atmospheric path with a reflection upon the Earth surface (Figure 1). The ground-based measurement inversion is, in principle, much more accurate than the space-based one because 1) it is not significantly affected by atmospheric scattering by aerosol or cloud which are known to be major sources of uncertainty for spaceborne measurements [*O'Brien and Rayner*, 2002], 2) the incoming signal level is larger by several order of magnitudes, which makes it possible to obtain high signal-to-noise ratio, 3) ground-based instruments are much larger than spaceborne sensors, so that higher spectral resolving power can be reached.

2.2. Generality on the Kitt Peak Instrument

[9] The spectral data are from the 1-m Fourier Transform Spectrometer (FTS) of the McMath-Pierce Solar telescope facility, which lies at the summit of Kitt Peak (32°N,

112°W, elev. 2095 m) in Arizona. The instrument, though mostly devoted to astronomical applications, is a powerful tool for the measurement of trace gas abundances in the atmosphere. The relatively remote location of the Kitt Peak site, about 60 miles southwest of Tucson, together with the limited vegetation coverage in the area, make the site mostly free from local influences so that atmospheric concentration measurements are representative of the background. The Kitt Peak FTS is capable of very high spectral resolution (0.01 cm^{-1}) measurements with broad spectral coverage (several thousands cm^{-1}).

[10] The high quality of the Kitt Peak measurements is achieved to the cost of systematic data averaging and rather long acquisition time. Each measured spectrum results from the Fourier transform of several (mostly 2 to 8) co-added interferograms, with individual time of acquisition on the order of 10 min. In consequence, there is a significant drift of the Solar Zenithal Angle (SZA) as the interferograms are being scanned and this causes complex distortion of the resulting Fourier transformed spectrum [*Kyle and Blatherwick*, 1984; *Park*, 1982]. In addition, the duration of the acquisition makes it difficult to unambiguously assign an effective SZA value to the measurement, which directly affects the accuracy of the mixing ratio retrievals through the airmass factor. This so-called smearing effect is particularly strong at low sun angles when the optical thickness of the atmosphere varies very much non-linearly with the SZA.

2.3. Radiative Transfer Model

[11] The forward simulation consists of a radiative transfer model of the atmosphere and a basic simulator of the Kitt Peak instrument spectral response. The radiative transfer model is based on a high computing resolution (5 10^{-4} cm^{-1}) multilayer, multispecies line-by-line code developed at Laboratoire des Sciences du Climat et de l'Environnement (LSCE). The model accounts for refractive ray tracing and the atmosphere sphericity. The vertical profiles of temperature and humidity were built on 16 levels of pressure using 4-times daily re-analysis by the NCEP model for the location and time of the Kitt Peak measurements. At Kitt Peak level, values of temperature and humidity were interpolated using measurements of surface pressure at the McMath-Pierce station. The radiative transfer simulations takes into account the 250 m optical path within the telescope. Spectral lines parameters were taken from the HITRAN 2000 compilation [*Rothman et al.*, 1998] for the 1.6-μm and 2.0-μm band. A recalculation of the O_2 line intensities by Goldman (personal communication, 2002) was used for the 1.27 μm band. Broadening of the CO_2 lines by the H_2O molecule was implemented in the form of the analytical quantum model by *Rosenmann et al.* [1988]. The atmospheric line shape was assumed to follow a Voigt function and was computed with the approximation by *Humlicek* [1978]. The airmass factor associated to the measurement was calculated as the average of the airmass factors at the zero path difference times of each raw interferograms [*Rinsland et al.*, 1984].

[12] The spectral response of the McMath-Pierce Fourier Transform Spectrometer was modeled by a non-damped cardinal sine function with a full-width-at-half-maximum set to the value of the spectral resolution reported in the ancillary data for each spectrum (typically between 0.01 cm^{-1} and 0.05 cm^{-1}). The spectra computed with a resolution of 5 10^{-4} cm^{-1} are convolved with the instrument response function.

2.4. Calibration Procedure

[13] As the differential absorption measurement is only sensitive to the relative depth of the absorption lines in the spectrum, there is no need for a calibration of the measurement amplitude. On the other hand, a wavelength drift of the measurement is clearly identified by the variable position of atmospheric absorption lines with respect to a reference spectrum. A spectral shift of the spectra is necessary for a good fit between models and measurements. Solar absorption lines are also apparent on the spectra, and their position vary with respect to those of the atmospheric lines. We determined the spectral shift of the measurements using a high-resolution (10^{-3} cm^{-1}) cross-correlation matching technique to a reference spectrum. Two different spectra were used to adjust the position of atmospheric and solar absorption lines. The reference solar spectrum is taken from the high resolution IR atlas by *Livingston and Wallace* [1991], while the atmospheric spectrum was computed using our radiative transfer model and an a priori state of the atmosphere.

[14] As an independent validation of the cross correlation technique, it was investigated whether the relative shift of the solar lines observed in the measurements was in agreement with a Doppler shift. The Doppler shift of the solar lines is driven by the relative motion of the sun along the line of sight of the Kitt Peak instrument. It was modeled as the sum of two components: one with an annual cycle related to the ellipticity of the earth orbit around the sun and the other with a daily cycle caused by the Earth spin. The comparison between the measured and the modeled spectral shifts in the 1.27-μm band (Figure 2) show an excellent agreement. The relative Doppler shift $\Delta\lambda/\lambda$ (where λ denotes the wavelength) is on the order of a few 10^{-6} and is retrieved in most cases to better than 5 10^{-7}. Note that such accuracy is significantly better than the measured spectra sampling ($\Delta\lambda/\lambda \approx 1.3\ 10^{-6}$).

2.5. Inversion of the Spectra

[15] The inversion model provides volume-mixing ratios (VMRs) of CO_2 and O_2 averaged along the instrument line of sight. This is achieved through a non linear least squares spectral fitting procedure [*Chang et al.*, 1978; *Niple et al.*, 1980] applied to the logarithm of the wavelength calibrated radiance L_λ [*Buchwitz et al.*, 2000]. In the current study, a total of 6 parameters are adjusted simultaneously for each spectrum. The inversion procedures seeks a best fit of the observed and modeled spectra:

$$L_\lambda \approx T_\lambda(x_{gas}, x_{H2O}) P_\lambda(a_0, a_1, a_2, a_3) \quad (1)$$

where T_λ is the modeled atmospheric transmission, P_λ is a low order polynomial and the various parameters are described below. Because, some of the adopted absorption lines are saturated at their center and may result in unfavorable signal-to-noise ratio, spectral intervals such that $T_\lambda < 10^{-2}$ are not used in the inversion procedure. We also filter out spectral intervals affected by solar lines as the latter are not reproduced by the forward model.

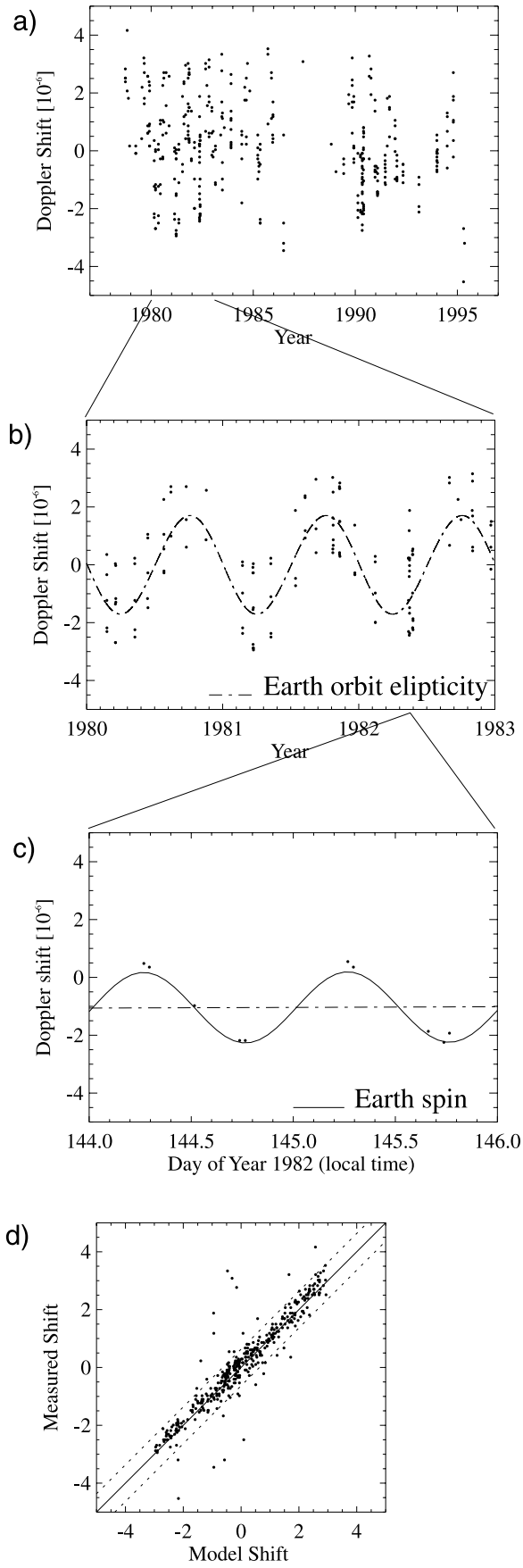

[16] The parameters x_{gas} and x_{H2O} are scale factors of the a priori VMR vertical profiles of the inversed gas, the vertical distribution of the gas concentration being fixed. The scale factor x_{gas} is for the targeted gas (i.e., either CO_2 or O_2) whereas the scale factor x_{H2O} is for H_2O whose absorption lines may interfere in the selected bands. The a priori vertical profile of CO_2 and O_2 are chosen uniform and are respectively attributed a VMR value of 350 10^{-6} and 0.295. The a priori profile of humidity is issued from meteorological re-analysis of the NCEP model for the location and time of the Kitt Peak measurements. The estimated column-averaged VMR is the product of the retrieved scale factor x_{gas} and the a-priori column-averaged VMR.

[17] The other four retrieved parameters a_0, a_1, a_2, a_3 are coefficients of a low order polynomial in the form $P(\lambda) = a_0 + a_1(\lambda - \lambda_0) + a_2(\lambda - \lambda_0)^2 + a_3(\lambda - \lambda_0)^3$ where λ is the wavelength and λ_0 is the central wavelength of the spectral interval. This polynomial is used to account for solar top-of-atmosphere spectral radiance, O_2 and H_2O absorption continua, whose spectral signatures are expected to be broadband over the limited spectral intervals that we adopt.

2.6. Validation With an Atmospheric Transport Model

[18] No vertical soundings of the atmospheric CO_2 above Kitt Peak exist to corroborate the atmospheric spectra inversions. *Yang et al.* [2002] have pointed out the strong similarity of their inversion results with the record of flask measurements at the Mauna Loa station. However, the reasons for this concordance remain ambiguous. First, the type of measurement differ radically between the two stations: the Mauna Loa measurements, although relatively high in altitude (3397 m), are mixing ratio relative to a given level whereas the Kitt Peak atmospheric spectra are representative of the vertically integrated content. Besides, the Mauna Loa and Kitt Peak sites are located far away, with significant differences in latitude (12.4°) and longitude (44.0°) between the two. These considerations have led us to attempt a validation of the Kitt Peak inversion results by use of simulated data.

[19] The Laboratoire de Météorologie Dynamique zoom (LMDz) 3D atmospheric transport model was used to simulate the evolution of the CO_2 content above Kitt Peak over the period of interest (1979–1995). The 3D simulation makes it possible to compute CO_2 column-averaged mixing ratio, with adequate weighting. The simulation used surface CO_2 fluxes obtained through an atmospheric inversion of surface concentration measurements by *Bousquet et al.* [2000] and was nudged to the

Figure 2. Comparison of measured and modeled Doppler shifts in the 1.27 μm band. The Doppler shift $\Delta\lambda/\lambda$ is measured from the relative displacement of solar and atmospheric absorption line on the observed spectra. The model accounts for the ellipticity of the Earth orbit around the Sun (Figure 2b) with a period of one year, and the Earth spin (Figure 2c) with a period of one day. The two effects have similar order of magnitude. Accounting for both effects yield an excellent agreement with the measurements (Figure 2d). In Figure 2d, the dashed lines correspond to the spectral sampling of the Kitt Peak spectra.

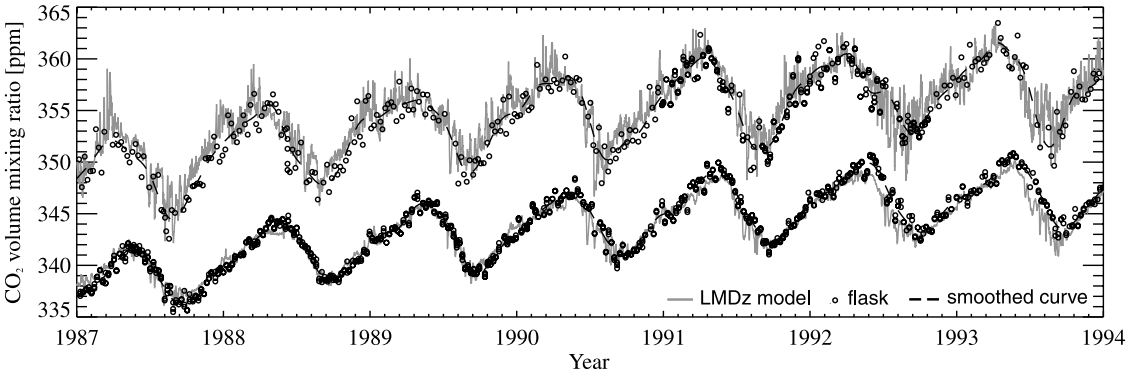

Figure 3. CO_2 volume mixing ratio at Niwot Ridge, (40.1N, 105.6W, elev. 3475 m) (above) and Mauna Loa, (19.5N, 155.6W, elev. 3397 m) (below) as simulated by the LMDz atmospheric transport model (gray line), compared to flask measurements at the two stations (black dots). The dashed curves are smoothed time series derived from the flask measurements [*Thoning et al.*, 1989]. The simulation is based on surface fluxes of CO_2 [*Bousquet et al.*, 2000] estimated from the inversion of concentration measurements that include the Mauna Loa and Niwot Ridge measurements. The Mauna Loa time series have been shifted down by 10 ppm for the sake of clarity.

ECMWF re-analysis meteorology over that period. Although the model is certainly imperfect due in particular to its low horizontal/vertical resolution (96 × 72 grid cells, 19 levels), uncertainties in the air mass transport and unresolved CO_2 surface flux characteristics, it matches the monthly means of surface measurements of CO_2 concentration at 76 sampling stations over the time period of interest. Note that the diurnal cycle of the biospheric CO_2 fluxes was not taken into account in the simulation, a non-critical simplification if the objective is to compare vertically integrated contents.

[20] We first want to assess the uncertainty in the model simulation. Figure 3 compares the 3-hourly averaged modeled mixing ratio with the flask sample measurements over a period of seven years at two observation sites, Niwot Ridge, a continental station located 1000 km to the North-East of Kitt Peak, and Mauna Loa, in the middle of the Pacific Ocean. Note that both stations are located at a relatively high altitude, 3475 m and 3397 m respectively. As expected from the use of monthly inverted fluxes [*Bousquet et al.*, 2000], the model accurately reproduces the major characteristics of the flask samples time series. The growth rate, as well as the amplitude and phase of the seasonal cycle appear similar for the flask samples and model results. Once the short-term variations are smoothen, the differences do not exceed 1 ppm (see for instance May 92 and 93 over Mauna Loa).

[21] The two upper time series of Figure 4 are a zoom of Figure 3 over a 2-year period to allow a better analysis of the short-term "synoptic" variations. As indicated by the comparison of the flask sample measurements and a smoothed curve (calculated after the flask data as the sum of a third order polynomial, a series of four harmonic of the annual frequency and the 60-day filtered residuals from the fit to the flask data [*Thoning et al.*, 1989]), the amplitude of the synoptic variations are on the order of 2 ppm RMS at Niwot Ridge and 1 ppm RMS at Mauna Loa. The model time series show synoptic variations with

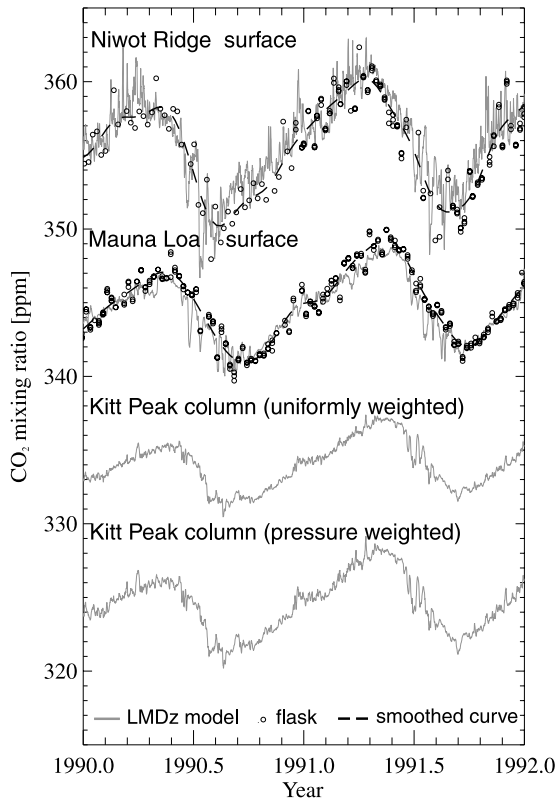

Figure 4. Measured and model CO_2 mixing ratios. The first and second time series are respectively the Niwot Ridge and Mauna Loa surface records of Figure 3 enlarged for the 1990–1991 period. The third and fourth time series show the model simulated column-averaged mixing ratio above Kitt Peak (31.9N, 111.6W, elev. 2070 m), with a uniform and pressure weighting respectively, for the same time period. The second, third and fourth time series have been shifted down by 10, 20 and 30 ppm respectively for the sake of clarity.

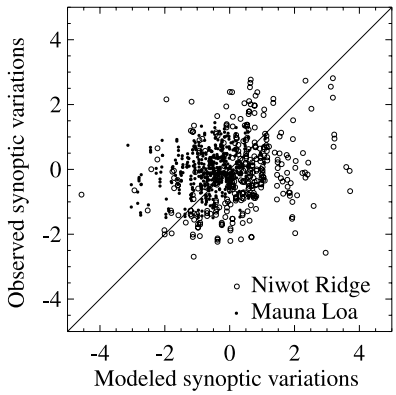

Figure 5. Short term variations of the simulated and measured CO_2 mixing ratio at Niwot Ridge and Mauna Loa shown in a scatterplot for the same time period as Figure 4. The X and Y axis data points have been obtained by subtracting the smoothed flask measurements time series from the model simulation and the flask measurements respectively.

the same amplitude. Note that, for the sake of clarity, we chose not to display the smoothed curves issued from the simulations as the latter are nearly identical to the smoothed curves calculated after the flask data.

[22] Figure 5 shows a scatterplot of the synoptic variations of the model and flask samples for the time period of Figure 4. The synoptic signal has been estimated by subtracting from the model/flask data the corresponding smoothed value. While there is no observed correlation between these data points, the spread is similar on the X and Y axis of the scatterplot. These results demonstrate that the phase of the synoptic variations is not well captured by the model but confirm that the predicted amplitude of the synoptic variability is in good agreement with that of the flask data at both stations (around 1 ppm RMS and 2 ppm RMS at Mauna Loa and Niwot Ridge respectively).

[23] The two lower plots of Figure 4 show the simulated time series of CO_2 column-averaged mixing ratio above Kitt Peak. Two types of vertical averaging have been computed with the 3D simulations, one with a uniform vertical weight, and another pressure weighted to reflect the weighting functions of the 1.6-μm and 2.0-μm band respectively [*Dufour and Bréon*, 2003]. According to the simulations, the synoptic variability of the column-averaged mixing ratios, both uniformly and pressure-weighted, is less than 1 ppm. Note that the pressure-weighted content shows larger synoptic variations than the uniformly weighted content. The former has a larger sensitivity to the lower atmospheric layer where the synoptic variability is larger.

[24] The relatively good agreement of the simulation with the flask measurements at the surface in the sectors of the Mauna Loa and Niwot Ridge stations (Figure 4) gives us some confidence in the reliability of the column-averaged mixing ratio simulated above Kitt Peak. One may trust the growth rate and seasonal signal of the time series predicted by the simulation. Besides, while the synoptic variations of the modeled column-averaged CO_2 mixing ratio above Kitt Peak are likely to be imprecise, their magnitude (1 ppm rms) can be essentially trusted. Indeed, although there is no possible validation of the LMDz model outputs against vertical soundings near the Kitt Peak observatory, we can reasonably assume that the model performances do not deteriorate when considering a column-integrated content rather than a surface content: short-term variability of the CO_2 concentrations, the most critical feature to simulate, usually decreases with altitude. Accordingly, we shall use the LMDz model simulation as a validation of our spectra inversions, bearing in mind that its uncertainty is on the order of 1 ppm rms.

3. Results

3.1. Data Selection

[25] We have analyzed a subset of 307 absorption spectra chosen among the data acquired with the Kitt Peak Fourier Transform spectrometer and available by anonymous ftp access to ftp://nsokp.nso.edu/FTS_cdrom/. The criteria of selection were the availability of the three spectral bands of interest. In addition, in order to limit the effect of smearing, only measurements with sun elevation higher than 9.6° (i.e., airmass factor less than 6) and duration of acquisition less than 40 min were retained. The data set covers a 18-year period between 1978 and 1996 on the basis of a few measurements per year. Note that, for the suitable days, several spectra are available, acquired at different times during daylight.

[26] The inversion model was applied to three narrow (15 cm^{-1} wide) spectral intervals lying within the 1.27-μm O_2 absorption band and the 1.6-μm and 2.0-μm CO_2 absorption bands. The spectral intervals were empirically chosen so as to cover a large number of significant absorption lines of the target species, free of perturbation by either solar or water vapor spectral features.

3.2. Spectral Fits

[27] Figure 6 shows an example of spectral fits in the three bands. The largest discrepancies between the modeled and the measured transmissions are on the order of a few percents and are usually observed in the vicinity of the absorption line centers. These spectral structures, which are highly systematic in the measurements, are most likely due to defects in the spectroscopic parameters (line intensity and width). However, other sources of error such as imperfect

Figure 6. (a, b, c) Comparison of measured (dots) and calculated (line) spectra after model inversion. The top panels show the modeled atmospheric transmission T_λ overlaid with the measured radiance L_λ divided by the retrieved low order polynomial P_λ (see equation 1). The bottom panels show their difference ($L_\lambda/P_\lambda - T_\lambda$) multiplied by 100. Data points that have not been used for the inversion (spectral intervals affected by solar lines or such that $T_\lambda < 10^{-2}$) are screened off. Figure 4a is the 2.0-μm CO_2 band, Figure 4b is for the 1.6-μm CO_2 band and Figure 4c is for the 1.27-μm O_2 band. The measurement was acquired on May 9, 1981, at an average SZA of 71°.

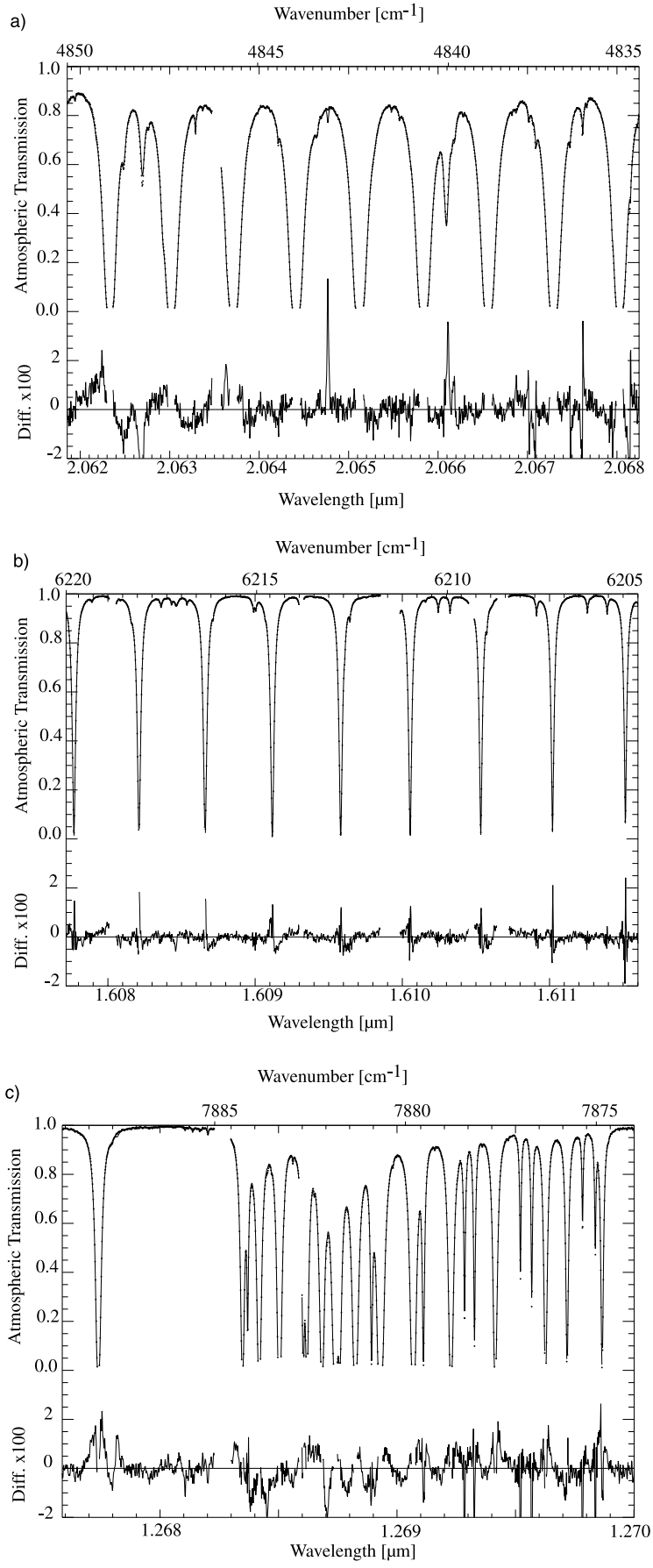
a)
Wavenumber [cm-1]
4850
4845
4840
4835
Atmospheric Transmission
Diff. x100
2.062
2.063
2.064
2.065
2.066
2.067
2.068
Wavelength [μm]
b)
Wavenumber [cm-1]
6220
6215
6210
6205
Atmospheric Transmission
Diff. x100
1.608
1.609
1.610
1.611
Wavelength [μm]
c)
Wavenumber [cm-1]
7885
7880
7875
Atmospheric Transmission
Diff. x100
1.268
1.269
1.270
Wavelength [μm]

Figure 6

knowledge of the profiles of temperature and humidity along the vertical or smearing of the spectral data may also contribute. In the non-absorbing regions, the measurement-model difference appears fully random and is attributed to measurement noise, with an amplitude on the order of 10^{-3}.

[28] Accounting for all the selected observations, the RMS spectral difference between the modeled and the measured atmospheric transmission spectra is around 1.0%, 0.3% and 0.7% for the 2.0-μm CO_2 band, the 1.6-μm CO_2 band and the 1.27-μm O_2 band respectively. There are several reasons for the relatively large error in the 2.0-μm CO_2 band. The latter suffers from contamination by water vapor absorption lines that are poorly reproduced by the model (the largest mismatches in the spectral residual of Figure 6a occur in the vicinity of the H_2O absorption lines). Besides, the 2.0-μm band has a relatively high sensitivity to temperature profile variability [*Dufour and Bréon*, 2003]. Finally, part of the errors at 2.0 μm may originate from the use of saturated lines. Indeed, the more intense an absorption line, the stronger its equivalent width (i.e., the total absorption that is fitted in the inversion) depends on the Lorentz width. Therefore the mismatches resulting from the uncertainties in the calculation of the Lorentz widths are expected to be larger at 2.0 μm than 1.6 μm.

3.3. Direct Retrievals

[29] Figure 7 shows the time series of the raw mixing ratio retrievals of CO_2 (from the 2.0-μm and 1.6-μm spectra) and O_2 (from the 1.27 μm spectra) over the full time period 1979–1995. There is a low bias for all three estimates, though of different magnitude between the bands. The mean absolute level of the CO_2 retrievals underestimates the mean value of the Kitt Peak simulated data by roughly 3% and 12% at 1.6 μm and 2.0 μm respectively. For the O_2 mixing ratios, the error is about 14% with respect to the expected value (0.2095). Note that the bias values were found to be very much dependent upon the choice of the 15 cm^{-1} spectral interval used for the inversion, an indication that the spectroscopic parameters show some variable error depending on the absorption lines.

[30] Both the 1.6 and 2.0-μm records show an increase in the CO_2 mixing ratio on the order of about 1.5 ppm per year, which is consistent with the expected long-term trend of CO_2 for the time period of the Kitt Peak measurements. On the other hand, the time series of CO_2 retrievals also show short-term variations up to 10 ppm peak to peak within the same day that are much larger than what can be expected from a diurnal cycle or synoptic events, as discussed in section 2.6.

[31] In the case of the O_2 column-averaged mixing ratio, the retrieved values are expected to be very stable, with no synoptic variations or trends (the latter are corrected for the surface pressure). The results show variations of several percents, with short-term variations as well as a general structure with an amplitude of almost 3% and a timescale of several years. This pluri-annual signal can be perceived in the CO_2 time series as well and is probably due to long-term drifts in the characteristics of the Kitt Peak instrument. The dispersion of the O_2 mixing ratio retrievals around their mean is roughly 2% rms, which is much larger than the actual variability of the concentration of oxygen in air.

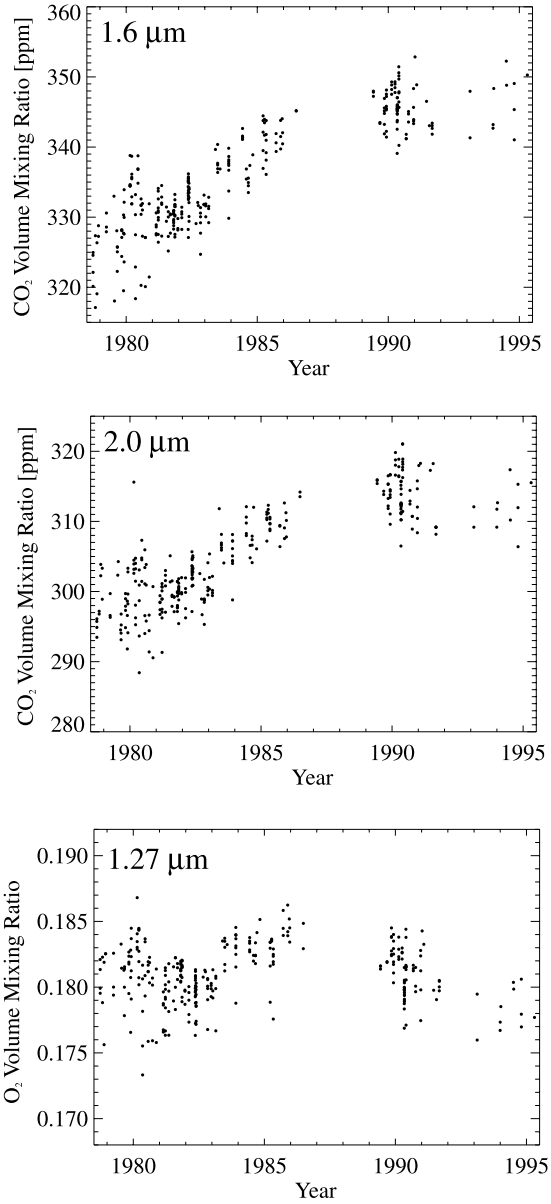

Figure 7. Result of mixing ratio inversions using the Kitt Peak spectra available for the period 1978–1995. The top and middle panels are for the CO_2 mixing ratio derived from the 1.6-μm and 2.0-μm bands respectively. The bottom panel is for the O_2 mixing ratio. The data points are the direct result of spectra inversion, with no correction or calibration. There is a clear low bias for all three retrievals.

Therefore the 2% value can be considered as a good estimate for the precision of the raw inversion results.

[32] A joint analysis of the three time series reveals that there is, in addition to the common pluri-annual structure, a strong correlation in the short-term variations of the CO_2 and O_2 data. These "inter-band" error correlations were also observed between the 1.6-μm CO_2 band and the 1.27-μm O_2 band in the [*Wallace and Livingston*, 1990] and [*Yang et al.*, 2002] studies, but there are only hypothesis for the exact cause(s) of these correlated errors. We believe that the short-term variation and its inter-band correlation result from the uncertainty on the effective airmass factor.

Indeed, the duration of the measurement implies some uncertainty on the airmass that is used to compute a concentration from the slant column.

3.4. Corrected Retrievals of CO_2 Mixing Ratio

[33] To overcome the air mass assignment errors, together with the calibration errors, it is proposed to use the O_2 mixing ratio retrieval to provide a constraint on the effective mass of dry air optically traversed. To the first order, one can expect these errors will impact all three mixing ratio retrievals by the same scale factor. This would therefore suggest an empirical correction in the form

$$r_{CO2}^{corr} = r_{CO2}^{meas} \times k \times \left(\frac{0.2095}{r_{O2}^{meas}}\right) \quad (2)$$

where r_{CO2}^{corr} is the corrected CO_2 mixing ratio retrieval, r_{CO2}^{meas} is the original CO_2 mixing ratio retrieval, r_{O2}^{meas} is the concomitant O_2 mixing ratio retrieval and k is a constant scale factor used to correct for the systematic biases in the mixing ratio retrieval of CO_2 and O_2 previously discussed. Note that the correction scheme depicted in equation (2) was adopted in the [*Wallace and Livingston*, 1990] and [*Yang et al.*, 2002] studies.

[34] Nevertheless, in practice, there is some variability between the bands on the effective mass of dry air optically traversed due to the non-linear relationship between the radiance and the mass of absorption material. We have accordingly chosen to apply a correction in the form

$$r_{CO2}^{corr} = r_{CO2}^{meas} \times k \times \left(\frac{0.2095}{r_{O2}^{meas}}\right)^{\alpha} \quad (3)$$

where the exponent α is used to correct for non linear effect between the adopted CO_2 and O_2 spectral intervals. The parameter k was assigned a value of 0.914 and 1.003 and the parameter α a value of 0.714 and 0.752 at 1.6 μm and 2.0 μm respectively. These values have been optimized based on a least squares minimization between the simulated and the retrieved CO_2 mixing ratio time series (not shown).

[35] In view of the corrected CO_2 retrievals time series (Figure 8), there is a substantial gain of precision in both bands. The seasonal cycle emerge clearly in both 1.6-μm and 2.0-μm time series. In addition, the long-term trends appear better reproduced. Finally, the intraday variability, though still present, is significantly reduced. Besides, the curves depicted by the Kitt Peak data points appear to be in good agreement with the atmospheric transport simulation over the same time period, with no visible difference in the form, amplitude and phase of the annual cycles. This is best demonstrated in the zoom (Figure 8, bottom panel) over the 9-year period with the highest temporal density of spectra measurements.

[36] The scatterplots of the retrieved and modeled CO_2 column-averaged mixing ratio (left panels of Figure 9) confirm the high degree of correlation between the two data sets in both bands. However, the signal in these scatterplots is mostly generated by the CO_2 general growth over the analyzed 16-year period. Clearly, we expect the CO_2 retrieval to reproduce more than the general trend. In order to explore how well the retrievals reproduce the CO_2 annual cycles, we have subtracted the simulation 2 year running average (dashed line in Figure 8) from the two data sets. After removal of the long-term trend, the data points remain relatively correlated in both bands (right panels of Figure 9), though with a coarser dispersion for the 2.0-μm

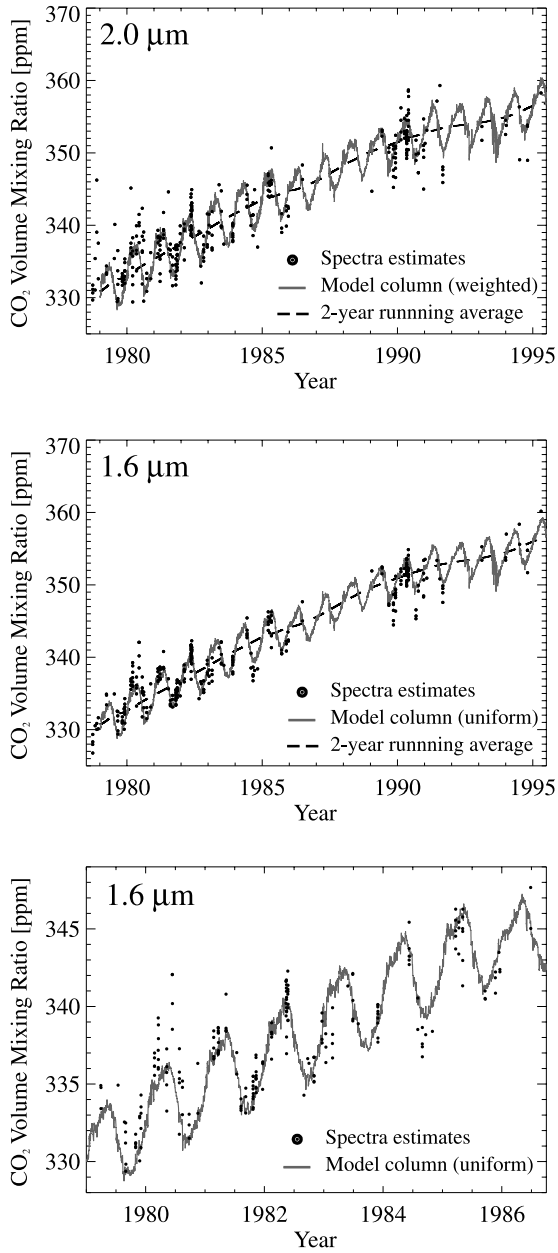

Figure 8. Time series of atmospheric CO_2 column mixing ratio above Kitt Peak derived from the spectral measurements (black dots) and simulated by the atmospheric transport model (gray curve). The dashed curve is a 2-year running average of the simulated times series. The CO_2 retrievals of Figure 7 have been corrected using the corresponding oxygen retrievals and scaled by a constant value to correct for systematic biases in the retrieval (see text). The top and middle panels show the results using the 2.0-μm and 1.6-μm band respectively. The bottom panel is an enlargement of the 1.6-μm results on the 1979–1986 period that shows the highest density of available spectra.

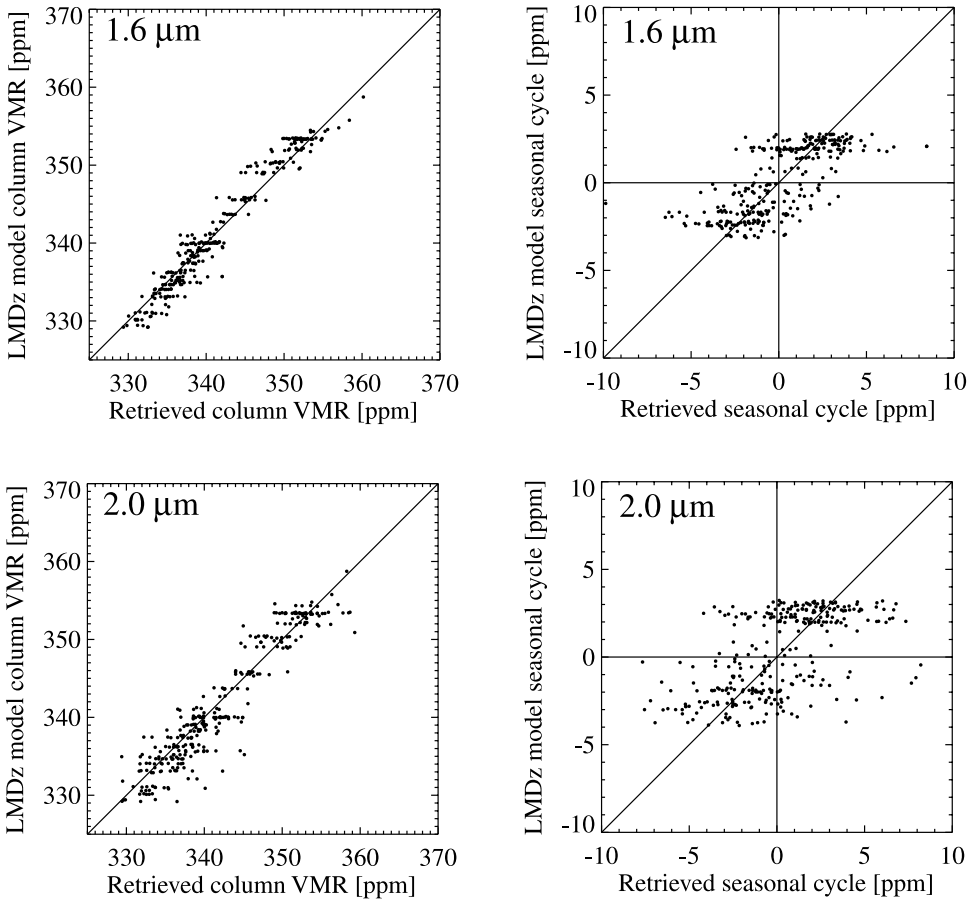

Figure 9. Scatterplot of the CO_2 column mixing ratio derived from spectral measurements and the simultaneous atmospheric transport model results. The points correspond to the same data as in Figure 8. The Figures to the left compare the spectra retrievals and coincident model results. The high correlation indicates that the two data sets show the same general trend over the time period. The Figures to the right are based on the same measurements, but after the 2-year running average of the simulated time series has been removed from the two data sets.

retrievals. These plots confirm that the CO_2 annual signal is being captured in the retrievals of both band.

[37] It is difficult to discern the part of noise and signal in the retrievals. Indeed, this would ideally require the knowledge of the actual column-averaged mixing ratio above Kitt Peak and in particular its synoptic components. Nevertheless, section 2.6 has shown that the uncertainty of the column-averaged mixing ratio derived from the LMDz model simulation, including that resulting from an erroneous phasing of the synoptic events, is most probably on the order of 1 ppm. Therefore any model-retrieval difference larger than 1 ppm should be interpreted as a noise in the retrievals. From the RMS differences computed on the data points of Figure 9, it is estimated that the RMS error on the 1.6-µm and 2.0-µm individual retrievals are respectively 1.5 ppm (or 0.4%) and 2.5 ppm (or 0.7%).

4. Conclusions

[38] This paper analyzes 307 solar spectra acquired from the Kitt Peak Fourier Transform spectrometer. The measurements are used to estimate the column-averaged mixing ratio of carbon dioxide using the differential absorption technique. There is clearly some information in the spectra as the general trend and the seasonal cycle of CO_2 atmospheric mixing ratios are depicted without ambiguity and consistent with independent simulations using an atmospheric transport model (LMDz) and optimized CO_2 surface fluxes [*Bousquet et al.*, 2000]. The RMS differences between the atmospheric transport model simulated data and the individual results of the spectra inversion are on the order of 1.5 ppm when using the 1.6-µm band and 2.5 ppm when using the 2.0-µm band. From a comparative analysis of the simulation results and flask samples time series at Mauna Loa and Niwot Ridge, it was estimated that the simulated column-averaged mixing ratio have an uncertainty that is likely to be close than 1 ppm. As a consequence, the RMS differences between the simulated columns and the inverted values must be attributed mostly to a noise in the latter.

[39] In this paper, we analyze in parallel the results derived from the 1.6 µm and 2.0 µm CO_2 absorption bands. It is of paramount importance to consider measurements in the 2.0-µm CO_2 band as a complement of the measurements in the 1.6-µm band in order to discriminate undesirable scattering effects from space [*Kuang et al.*, 2002] and

because of the relatively higher sensibility of the 2.0 μm band to the boundary layer [*Dufour and Bréon*, 2003] where the gradients of CO_2 concentrations are expected to be larger. Both the 1.6-μm and 2.0-μm bands will be used in the forthcoming OCO mission [*Crisp et al.*, 2002]. The 2.0-μm retrievals appear noisier than those obtained from 1.6-μm spectra. This could be expected from radiative transfer simulations that indicate a larger sensitivity to the uncertainty on the temperature profile and several spectroscopic parameters (air-broadened width and its coefficient of dependence as a function of temperature) as well as some contamination by water vapor absorption. As a consequence, it is not clear whether the 2.0-μm band provides additional information for a better retrieval that combines both band measurements.

[40] The demonstration is made that CO_2 column-averaged mixing ratio retrievals of the same individual accuracy as obtained by *Yang et al.* [2002] can be derived from narrow spectral bands that include only a few absorption lines. There is no need to sample the full CO_2 absorption band, which potentially makes the measurements faster and may be exploited to design spaceborne sensors with shorter acquisition times or higher signal-to-noise ratio.

[41] Although there is clearly some CO_2 information in the spectra, the study also raises a number of unresolved questions. The mixing ratio retrievals show a significant low bias. This is most probably the result of inaccuracies in the absorption line intensities. More worrisome is the need for empirical correction by the oxygen mixing ratio. The most likely hypothesis for the efficiency of the correction is the uncertainty in effective airmass, a result of the rather long duration of acquisition scans. Even after the correction, an error on the CO_2 column-averaged mixing ratio remains. The residual error may result from the uncertainty on the effective airmass, as its effect is not necessarily the same in all three mixing ratio retrievals. Although possible, we have no demonstration that this uncertainty, which could be reduced by shorter acquisitions, is indeed the main source of error. Therefore at this point, there is no empirical demonstration that the CO_2 column can be retrieved with an accuracy of 1 ppm, even from rather favorable direct sun spectra measurements.

[42] **Acknowledgments.** The authors would like to thank CNES and European-Union (COCO project, EVG1-CT2001-00056) for financial support. We are indebted to the Kitt Peak National Solar Observatory, which is operated by the Association of Universities for Research in Astronomy, under a cooperative agreement with the National Science Foundation. We are particularly grateful to D. Brantson, M. Dulick, and C. Plymate from NOAO, who provided precious information and advice on the McMath-Pierce solar telescope measurements. Finally, we acknowledge valuable discussions and contributions from C. Camy-Peyret from CNRS/University Paris 6 and G. C. Toon of California Institute of Technology.

References

Bousquet, P., P. Peylin, P. Ciais, C. Le Quere, P. Friedlingstein, and P. P. Tans (2000), Regional changes in carbon dioxide fluxes of land and oceans since 1980, *Science*, *290*(5495), 1342–1346.

Buchwitz, M., V. V. Rozanov, and J. P. Burrows (2000), A near-infrared optimized DOAS method for the fast global retrieval of atmospheric CH_4, CO, CO_2, H_2O, and N_2O total column amounts from SCIAMACHY Envisat-1 nadir radiances, *J. Geophys. Res.*, *105*(D12), 15,231–15,245.

Chang, Y. S., J. H. Shaw, J. G. Calvert, and W. M. Uselman (1978), Determination of abundances of gases from solar spectra, *J. Quant. Spectrosc. Radiat. Transfer*, *19*(6), 599–605.

Crisp, D., et al. (2002), *The Orbiting Carbon Observatory* (*OCO*) *Mission*, Com. on Space Res., Houston, Tx.

Dufour, E., and F.-M. Bréon (2003), Spaceborne estimate of atmospheric CO_2 column by use of the differential absorption method: Error analysis, *Appl. Opt.*, *42*(18), 3595–3609.

Farmer, C. B., O. F. Raper, B. D. Robbins, R. A. Toth, and C. Muller (1980), Simultaneous spectroscopic measurements of stratospheric species: O_3, CH_4, CO, CO_2, N_2O, H_2O, HCl, and HF at northern and southern mid-latitudes, *J. Geophys. Res.*, *85*, 1621–1632.

GLOBALVIEW-CO_2 (2000), *Cooperative Atmospheric Data Integration Project: Carbon Dioxide*, NOAA, Boulder, Colo.

Humlicek, J. (1978), An efficient method for evaluation of the complex probability function: The Voigt function and its derivatives, *J. Quant. Spectrosc. Radiat. Transfer*, *21*, 309–313.

Kuang, Z. M., J. Margolis, G. Toon, D. Crisp, and Y. Yung (2002), Spaceborne measurements of atmospheric CO_2 by high-resolution NIR spectrometry of reflected sunlight: An introductory study, *Geophys. Res. Lett.*, *29*(15), 1716, doi:10.1029/2001GL014298.

Kyle, T. G., and R. Blatherwick (1984), Smearing of interferograms in Fourier transform spectroscopy, *Appl. Opt.*, *23*(2), 261–263.

Livingston, W., and L. Wallace, (1991), An atlas of the solar spectrum in the infrared from 1850 to 9000 cm^{-1}, *Natl. Sol. Obs. Tech. Rep., 91-001*.

Niple, E., W. G. Mankin, A. Goldman, D. G. Murcray, and F. J. Murcray (1980), Stratospheric NO_2 and H_2O mixing ratio profiles from high resolution infrared solar spectra using nonlinear least squares, *Geophys. Res. Lett.*, *7*(7), 489–492.

O'Brien, D. M., and P. J. Rayner (2002), Global observations of the carbon budget - 2. CO_2 column from differential absorption of reflected sunlight in the 1.61 μm band of CO_2, *J. Geophys. Res.*, *107*(D18), 4354, doi:10.1029/2001JD000617.

Park, J. H. (1982), Effect of interferogram smearing on atmospheric limb sounding by Fourier transform spectroscopy, *Appl. Opt.*, *21*(8), 1356–1366.

Park, J. H., J. M. Russell, and M. A. H. Smith (1980), Solar occultation sounding of pressure and temperature using narrowband radiometers, *Appl. Opt.*, *19*(13), 2132–2139.

Rayner, P. J., and D. M. O'Brien (2001), The utility of remotely sensed CO_2 concentration data in surface source inversions, *Geophys. Res. Lett.*, *28*, 175–178.

Rinsland, C. P., R. E. Boughner, J. C. Larsen, G. M. Stokes, and J. W. Brault (1984), Diurnal variations of atmospheric nitric oxide: Ground-based infrared spectroscopic measurements and their interpretation with time-dependent photochemical model calculations, *J. Geophys. Res.*, *89*, 9613–9622.

Rosak, A., and F. Tintó, (2003), Static Fourier transform spectrometer for CO2 monitoring, paper presented at 30th International Symposium on Remote Sensing of Environment (ISRSE), Int. Cent. for Remote Sens. of the Environ., Honolulu, Hawai'i.

Rosenmann, L., J. M. Hartmann, M. Y. Perrin, and J. Taine (1988), Accurate calculated tabulations of IR and Raman CO_2 line broadening by CO_2, H_2O, N_2, O_2 in the 300–2400 K temperature range, *Appl. Opt.*, *27*(18), 3902–3907.

Rothman, L. S., et al. (1998), The HITRAN molecular spectroscopic database and HAWKS (HITRAN Atmospheric Workstation): 1996 edition, *J. Quant. Spectrosc. Radiat. Transfer*, *60*(5), 665–710.

Schimel, D. S., et al. (2001), Recent patterns and mechanisms of carbon exchange by terrestrial ecosystems, *Nature*, *414*(6860), 169–172.

Thoning, K. W., P. P. Tans, and W. D. Komhyr (1989), Atmospheric carbon dioxide at Mauna Loa Observatory, 2, Analysis of the NOAA GMCC data, 1974, 1985, *J. Geophys. Res.*, *94*, 8549–8565.

Tolton, B. T., and D. Plouffe (2001), Sensitivity of radiometric measurements of the atmospheric CO_2 column from space, *Appl. Opt.*, *40*(9), 1305–1313.

Wallace, L., and W. Livingston (1990), Spectroscopic observations of atmospheric trace gases over Kitt Peak: 1. Carbon dioxide and methane from 1979 to 1985, *J. Geophys. Res.*, *95*(D7), 9823–9827.

Yang, Z. H., G. C. Toon, J. S. Margolis, and P. O. Wennberg (2002), Atmospheric CO_2 retrieved from ground-based near IR solar spectra, *Geophys. Res. Lett.*, *29*(9), 1339, doi:10.1029/2001GL014537.

E. Dufour and F.-M. Bréon, Laboratoire des Sciences du Climat et de l'Environnement, Direction des Sciences de la Matière, Commissariat à l'Energie Atomique, F-91191 Gif sur Yvette, France. (dufour@lsce.saclay.cea.fr; breon@lsce.saclay.cea.fr)

P. Peylin, Laboratoire de Biogéochimie des Milieux Continentaux, INRA Grignon, F-78850 Thiverval-Grignon, France. (philippe.peylin@grignon.inra.fr)